Fermi National Accelerator Laboratory

FERMILAB-PUB-06-093-AD (2006)

Determination of linear optics functions from turn-by-turn data

Y.Alexahin, E.Gianfelice-Wendt

Fermi National Accelerator Laboratory
P.O. Box 500, Batavia, Illinois 60510

Abstract

A method for evaluation of coupled optics functions, detection of strong perturbing elements, determination of BPM calibration errors and tilts using turn-by-turn (TBT) data is presented as well as the new version of the Hamiltonian perturbation theory of betatron oscillations the method is based upon. An example of application of the considered method to the Tevatron is given.

(*Submitted to Physical Review Special Topics – Accelerators and Beams*)

May 2, 2006

PACS code: 29.27.-a

1 INTRODUCTION

Detail knowledge of the beam optics is crucial for successful performance of an accelerator. It is important to have tools for measurement and correction of beta-beating, coupling, for detection of sources of optics imperfections.

There are a number of methods to address these problems which can be classified into two major categories. The first one comprises methods based on driving the closed orbit motion (differential orbits [1], AC dipole [2]), while the others exploit free betatron oscillations excited by a kicker or injection errors.

The method considered in the present paper belongs to the second category and involves analysis of turn-by-turn beam position into normal modes of betatron oscillations. To do this we may Fourier analyze the data or try to fit it with a superposition of a limited number of harmonic oscillators. The second approach with simultaneous use of data from all available BPMs leads to the so-called *Independent Component Analysis* [3]. In the case of weakly coupled motion and low level of noise the Fourier analysis which we use here is no less efficient but significantly faster.

An important question is what representations of lattice functions to use. Many authors [4, 5, 6] employ the Edwards-Teng parameterization of the transfer matrix [7]. However, the Mais-Ripken parameterization [8] is more suitable for analysis of TBT data since it explicitly deals with the normal modes of coupled oscillations. We use the language of the transfer matrix eigenvectors which are closely related to the Mais-Ripken lattice functions (see e.g. Ref.[9]) and treat the expansion coefficients as new dynamic variables (normal forms) [10, 11]. In Section 2 we briefly remind the necessary formalism.

In principle, no *a priori* conception of the machine optics is necessary for analysis of TBT data. In Section 3 we discuss how to perform the *Model Independent Analysis*, though do not use it directly for practical calculations.

In practice there is always some ideal (design) optics which can be used as the starting point, the goals of the measurements being to find deviations from the ideal optics (e.g. beta-beating, "tilt" of the normal modes), detect the sources of perturbation, evaluate their strength and necessary changes in correction circuits to compensate for these perturbations.

These goals require different conditions of the measurements. It is easier to search for the optics imperfections and their sources when the tunes are sufficiently far from resonance values, whereas for evaluation of the global effects (e.g. closest tune approach which is essentially the absolute value of the difference resonance driving term) it is better to put the tunes close to the resonance.

In the near-resonance case the relation between the source strength and the observable effects of perturbation is nonlinear, so that the higher-order perturbation theory should be invoked. We put the details of such theory (based on the general Hamiltonian perturbation theory as presented in Ref.[11]) in Appendix A.

Application of the developed methods, including evaluation of possible BPM tilts and calibration errors is discussed in Section 4 and exemplified by the case of the Tevatron collision optics.

Error estimates are given in Appendices B and C. It is shown that in the presence of random noise the tune error decreases with the number of turns N only as $1/N^{3/2}$. Appendix B presents also an improved interpolation formula for precise tune determination using discrete Fourier transform.

2 DESCRIPTION OF COUPLED LINEAR MOTION

First let us introduce notation conventions: underlined characters will denote (column) phase space vectors, upright capital letters designate matrices, bilinear forms of dynamic variables (such as Hamiltonian) will be denoted in cursive.

We choose the generalized azimuth $\theta = s/R$ as independent variable (R and s being the machine average radius and the path length), and

$$\underline{z} = (x,\ x' - \frac{B_s}{2B\rho}\, y,\ y,\ y' + \frac{B_s}{2B\rho}\, x)^T \tag{2.1}$$

as the phase space vector, the prime denotes differentiation by s (we will use the dot for differentiation by θ) and superscript T means transposition.

In linear Hamiltonian systems considered in the present report the Hamiltonian is a bilinear function of dynamic variables

$$\mathcal{H}(\underline{z},\theta) = \mathcal{H}_0 = \frac{1}{2}\,\underline{z}^T\, \mathrm{H}_0(\theta)\underline{z} \tag{2.2}$$

with symmetric matrix H_0. The equations of motion can be written in the form

$$\dot{\underline{z}} = \mathrm{S}\frac{\partial}{\partial \underline{z}}\mathcal{H} = \mathrm{S}\mathrm{H}_0\,\underline{z} \tag{2.3}$$

where

$$\mathrm{S} = \mathrm{S}_2 \oplus \mathrm{S}_2, \quad \mathrm{S}_2 = \begin{pmatrix} 0 & 1 \\ -1 & 0 \end{pmatrix}. \tag{2.4}$$

The phase space vectors at two locations θ_1, θ_2 are related via transfer matrix $\mathrm{M}(\theta_2, \theta_1)$:

$$\underline{z}(\theta_2) = \mathrm{M}(\theta_2, \theta_1)\ \underline{z}(\theta_1), \tag{2.5}$$

which satisfies the equation

$$\frac{d}{d\theta}\mathrm{M}(\theta,\theta_0) = \mathrm{S}\mathrm{H}_0\mathrm{M}(\theta,\theta_0) \tag{2.6}$$

It is easy to verify by differentiation that the transfer matrix satisfies the symplecticity condition:

$$\mathrm{M}^T\mathrm{S}\mathrm{M} = \mathrm{S}, \tag{2.7}$$

2.1 Eigenvectors of the transfer matrix

Of special importance is the eigensystem of the 1-turn transfer matrix (from θ to $\theta + 2\pi$)

$$\lambda_n\, \underline{v}_n(\theta) = \mathrm{M}(2\pi + \theta, \theta)\ \underline{v}_n(\theta). \tag{2.8}$$

The eigenvalues λ_n form reciprocal pairs [9] and, outside the stopbands of half-integer and sum resonances, lie on a unit circle. We will numerate and arrange them in the following order:

$$\lambda_1 = \exp(2\pi i Q_1),\ \lambda_{-1} = \lambda_1^*,\ \lambda_2 = \exp(2\pi i Q_2),\ \lambda_{-2} = \lambda_2^*, \tag{2.9}$$

Equation (2.8) defines an eigenvector up to a (complex) constant. It is natural (but by no means necessary) to impose the condition

$$\underline{v}_{-n} = \underline{v}_n^*,\ n = 1, 2. \tag{2.10}$$

To write down the orthonormality condition let us build a matrix, V, using the eigenvectors as its columns:

$$V_{ik} = (\underline{v}_{n_k})_i \tag{2.11}$$

where n_k, $k = 1,\ldots, 4$ is the sequence 1, -1, 2, -2. Now we can write the orthonormality condition as

$$\mathrm{V}^T \mathrm{S}\, \mathrm{V} = -i\mu\, \mathrm{S}, \tag{2.12}$$

where the normalization constant μ must be real owing to condition (2.10), our choice being $\mu = 2$.

This condition still leaves the phases of eigenvectors $\underline{v}_n$ undefined and we can use this freedom to our best advantage. First we require that at the origin ($\theta = 0$) the spatial components $(\underline{v}_1)_1$ and $(\underline{v}_2)_3$ be real. To define the phases at other locations let us notice that by propagating an eigenvector from θ_1 to θ_2 with transfer matrix $\mathrm{M}(\theta_2, \theta_1)$ we get the eigenvector at θ_2 which corresponds to the same eigenvalue. Multiplying by exponentials $\exp(-iQ_n\theta)$ we can make the eigenvectors 2π-periodic:

$$\underline{v}_n(\theta) = e^{-iQ_n\theta}\, \mathrm{M}(\theta, 0)\, \underline{v}_n(0), \quad n = 1, 2, \tag{2.13}$$

or, in the matrix form,

$$\mathrm{V}(\theta) = \mathrm{M}(\theta, 0)\, \mathrm{V}(0) \Lambda(-\theta), \tag{2.14}$$

where

$$\Lambda(\theta) = \mathrm{diag}(e^{iQ_1\theta}, e^{-iQ_1\theta}, e^{iQ_2\theta}, e^{-iQ_2\theta}). \tag{2.15}$$

With this convention the transfer matrix can be expressed via the eigenvectors as

$$\mathrm{M}(\theta_2, \theta_1) = -\frac{i}{\mu} \mathrm{V}(\theta_2) \Lambda(\theta_2 - \theta_1)\, \mathrm{S}\, \mathrm{V}^T(\theta_1)\, \mathrm{S}. \tag{2.16}$$

Let us note for later reference that by differentiating eq.(2.14) we can obtain a differential equation for matrix V,

$$\dot{\mathrm{V}} = \mathrm{S}\mathrm{H}_0 \mathrm{V} - i\, \mathrm{V}\, \mathrm{Q}, \tag{2.17}$$

where $\mathrm{Q} = \mathrm{diag}(Q_1, -Q_1, Q_2, -Q_2)$.

2.2 Complex canonical variables (normal forms)

The phase space vector (2.1) can be expanded in eigenvectors with coefficients satisfying the relations $a_{-n} = a_n^*, \quad n = 1, 2$ by virtue of condition (2.10). In the matrix form the expansion reads

$$\underline{z} = \mathrm{V}(\theta)\, \underline{a}, \tag{2.18}$$

where we introduced vector of coefficients $\underline{a} = (a_1, a_1^*, a_2, a_2^*)^T$ which may be regarded as a new phase space vector [10, 11]. The inverse transformation is given by

$$\underline{a} = -\frac{i}{\mu} \mathrm{S}\, \mathrm{V}^T(\theta)\, \mathrm{S}\, \underline{z}. \tag{2.19}$$

According to eqs.(2.14) and (2.18) coefficients a_n propagate as

$$a_n(\theta) = e^{iQ_n\theta} a_{n0}, \tag{2.20}$$

so that the introduced variables are in the normal form.

Though matrix V is not symplectic when $\mu \neq i$, transformation (2.18) is still canonical in the sense that coefficients a_n, a_n^* form canonical pairs satisfying Hamilton's equations

$$\dot{a}_n = \frac{\partial}{\partial a_n^*} \mathcal{U}, \quad \dot{a}_n^* = -\frac{\partial}{\partial a_n} \mathcal{U}, \quad n = 1, 2, \quad \text{or} \quad \dot{\underline{a}} = \mathrm{S} \frac{\partial}{\partial \underline{a}} \mathcal{U} \tag{2.21}$$

with Hamiltonian

$$\mathcal{U} = \mathcal{U}_0 = i \sum_{n=1,2} Q_n a_n a_n^* \,. \tag{2.22}$$

Let us show that the equations for a_n retain the Hamiltonian form (2.21) even in the presence of perturbations when the transfer matrix M generated by unperturbed Hamiltonian $\mathcal{H}_0$ and its eigenvectors no longer describe the exact motion but still are used in transformation (2.18). Namely, let the Hamiltonian $\mathcal{H}(\underline{z}, \theta) = \mathcal{H}_0 + \mathcal{H}_1$ be a sum of unperturbed part $\mathcal{H}_0$ given by eq.(2.2) and perturbation $\mathcal{H}_1$ (which may contain terms of higher order in $\underline{z}$ as well).

Differentiating eq.(2.18) and using the inverse of eq.(2.12) and eq.(2.17) we get

$$\begin{aligned} \dot{\underline{a}} &= \mathrm{V}^{-1}(\dot{\underline{z}} - \dot{\mathrm{V}}\,\underline{a}) = \mathrm{V}^{-1}\mathrm{S}[\mathrm{H}_0\mathrm{V}\,\underline{a} + (\mathrm{V}^{-1})^T \frac{\partial}{\partial \underline{a}} \mathcal{H}_1] - \mathrm{V}^{-1}(\mathrm{S}\mathrm{H}_0\mathrm{V} - i\,\mathrm{V}\mathrm{Q})\underline{a} \\ &= \frac{i}{\mu}\mathrm{S}\frac{\partial}{\partial \underline{a}}\mathcal{H}_1 + i\,\mathrm{Q}\,\underline{a} = \mathrm{S}\frac{\partial}{\partial \underline{a}}\mathcal{U} \end{aligned} \tag{2.23}$$

so that a_n, a_n^* are still canonical variables and the transformed Hamiltonian is $\mathcal{U} = \mathcal{U}_0 + \mathcal{U}_1$ with unperturbed part $\mathcal{U}_0$ given by eq.(2.22) and

$$\mathcal{U}_1(\underline{a}, \theta) = \frac{i}{\mu}\mathcal{H}_1(\underline{z}, \theta)\big|_{\underline{z}=\mathrm{V}(\theta)\underline{a}} \tag{2.24}$$

Relations (2.18, 2.21-24) are general ones and can be used in analysis of nonlinear systems as well; the choice of normalization constant μ being the matter of personal preference. For the following we set $\mu = 2$.

2.3 Uncoupled lattice functions

In the absence of coupling the transfer matrix splits into a direct sum of 2×2 matrices which eigenvectors can be parameterized as follows:

$$\underline{v}_n(\theta) = e^{i\phi_n}\begin{pmatrix} \sqrt{\beta_n} \\ \dfrac{i - \alpha_n}{\sqrt{\beta_n}} \end{pmatrix}, \quad \underline{v}_{-n} = \underline{v}_n^*, \quad n = 1, 2\,, \tag{2.25}$$

where $\phi_n = \varphi_n - Q_n\theta$ is periodic phase function, α_n and β_n are the Twiss functions for mode n (in the following we assume mode 1 to be nearly horizontal and mode 2 to be nearly vertical).

For the transfer matrix we have the well known expression which we cite for later reference:

$$\mathrm{M}^{(n)}(\theta_k, \theta_j) = \begin{pmatrix} \sqrt{\dfrac{\beta_n^{(k)}}{\beta_n^{(j)}}}(\cos\Delta\varphi_n + \alpha_n^{(j)}\sin\Delta\varphi_n) & \sqrt{\beta_n^{(j)}\beta_n^{(k)}}\sin\Delta\varphi_n \\ -\dfrac{(1+\alpha_n^{(j)}\alpha_n^{(k)})\sin\Delta\varphi_n - (\alpha_n^{(j)} - \alpha_n^{(k)})\cos\Delta\varphi_n}{\sqrt{\beta_n^{(j)}\beta_n^{(k)}}} & \sqrt{\dfrac{\beta_n^{(j)}}{\beta_n^{(k)}}}(\cos\Delta\varphi_n - \alpha_n^{(k)}\sin\Delta\varphi_n) \end{pmatrix}, \tag{2.26}$$

where $\Delta\varphi_n = \varphi_n^{(k)} - \varphi_n^{(j)}$, superscripts j, k mark locations at which the lattice functions were taken.

2.4 Coupled lattice functions

In the case of coupled motion we use the modification of Mais-Ripken parameterization which was proposed by Lebedev and Bogacz[1] (see Ref.[12]):

$$\underline{v}_1(\theta) = \{e^{i\phi_{x1}}\sqrt{\beta_{x1}}\,,\, e^{i\phi_{x1}}\frac{i(1-\omega)-\alpha_{x1}}{\sqrt{\beta_{x1}}}\,,\, e^{i\phi_{y1}}\sqrt{\beta_{y1}}\,,\, e^{i\phi_{y1}}\frac{i\omega-\alpha_{y1}}{\sqrt{\beta_{y1}}}\}^T\,,$$
$$\underline{v}_2(\theta) = \{e^{i\phi_{x2}}\sqrt{\beta_{x2}}\,,\, e^{i\phi_{x2}}\frac{i\omega-\alpha_{x2}}{\sqrt{\beta_{x2}}}\,,\, e^{i\phi_{y2}}\sqrt{\beta_{y2}}\,,\, e^{i\phi_{y2}}\frac{i(1-\omega)-\alpha_{y2}}{\sqrt{\beta_{y2}}}\}^T\,. \tag{2.27}$$

2.5 Edwards-Teng parameterization

For the sake of completeness let us mention the Edwards-Teng parameterization which historically appeared first [7]. At every location in the ring the 1-turn transfer matrix $M(\theta+2\pi,\theta)$ can be transformed into the block-diagonal form by similarity transformation $\tilde{M} = RMR^{-1}$ with matrix $R=R(\theta)$ of the type

$$R = \begin{pmatrix} I\cos\Phi & -D^{-1}\sin\Phi \\ D\sin\Phi & I\cos\Phi \end{pmatrix} \tag{2.28}$$

where I is 2×2 identity matrix and $D=D(\theta)$ is some 2×2 symplectic matrix.

The eigenvectors of the decoupled transfer matrix $\tilde{M}$ are direct sums $\underline{v}_1 \oplus \underline{0}$, $\underline{0} \oplus \underline{v}_2$ and their complex conjugates with $\underline{v}_n$ being of the form (2.25) and $\underline{0} = (0, 0)^T$.

Lebedev and Bogacz [12] established relations between the Edwards-Teng and Mais-Ripken lattice functions. Namely, they showed that the phase advances coincide ($\varphi_1 = \varphi_{x1}$, $\varphi_2 = \varphi_{y2}$), while the β- functions are related as

$$\beta_1 = \frac{\beta_{x1}}{1-\omega}, \quad \beta_2 = \frac{\beta_{y2}}{1-\omega}. \tag{2.29}$$

For the "symplectic rotation" angle Φ they found

$$\sin^2\Phi = \omega \tag{2.30}$$

Though many authors [4, 5, 6] employ the Edwards-Teng parameterization, we prefer to work with the Mais-Ripken functions since they are immediately related to particle coordinates.

3 MODEL-INDEPENDENT ANALYSIS OF TBT DATA

In principle the lattice functions can be found from TBT data without resorting to the perturbation analysis, so that no *a priori* conception of the machine optics is necessary.

First of all, the normal mode tunes Q_1, Q_2 should be found using continuous Fourier transform or interpolated FFT as discussed in Appendix B (data from one BPM per plane is usually sufficient). To proceed further let us note that the generalized azimuth $\theta = s/R$ plays two roles: it marks locations

[1] An important step made by Lebedev and Bogacz was to show explicitly how Mais-Ripken's γ-functions can be expressed via α- and β- functions. They introduced an auxiliary function, denoted here as ω, which makes the expressions much simpler.

around the ring ($0 \le \theta_0 < 2\pi$) and serves as continuously advancing independent variable taking value $\theta = \theta_0 + 2\pi(k - 1)$ on k^{th} turn at location θ_0.

Taking into account eqs.(2.18) and (2.20) we expect the turn-by-turn beam position at j^{th} BPM location to be given by

$$x_{jk} = \sum_{m=1,2} \mathrm{V}_{1m}(\theta_j) a_{m0} e^{iQ_m[\theta_j + 2\pi(k-1)]} + c.c. \tag{3.1}$$

The vertical displacement can be expressed analogously via the 3rd components of the eigenvectors.

The Fourier components of the beam position (3.1) at the normal mode tunes are immediately related to the spatial components of eigenvectors:

$$\begin{aligned} X_j(Q_m) &= \frac{1}{N}\sum_{k=1}^{N} x_{jk} e^{-2\pi i Q_m(k-1)} = V_{1m}(\theta_j) a_{m0} e^{iQ_m\theta_j} + O(\frac{1}{N}), \quad j = 1,..., N_h \\ Y_l(Q_m) &= \frac{1}{N}\sum_{k=1}^{N} y_{lk} e^{-2\pi i Q_m(k-1)} = V_{3m}(\theta_l) a_{m0} e^{iQ_m\theta_l} + O(\frac{1}{N}), \quad l = 1,..., N_v \end{aligned} \tag{3.2}$$

where N_h and N_v are the numbers of horizontal and vertical BPMs respectively.

Recalling definitions (2.11) and (2.27) we get for the horizontal Mais-Ripken optics functions at horizontal BPMs

$$\beta_{xm}(\theta_j) = | X_j(Q_m) / a_{m0} |^2, \quad \varphi_{xm}(\theta_j) = \arg[X_j(Q_m) / a_{m0}], \quad m = 1, 2, \tag{3.3}$$

and analogously for the vertical functions at vertical BPMs.

We may apply formulas (3.2), (3.3) to the real data (error estimates are given in Appendix C). The remaining question is how to find the invariant amplitudes $|a_{m0}|$, the argument of a_{m0} not being an issue since the betatron phase is defined up to a constant addend.

3.1 Determination of the invariant amplitudes

The difficulty is that the invariant amplitude of oscillations is determined not only by the kick strength but also by the optics functions yet to be found. Provided the BPMs sample the ring densely enough there is a principal solution which can be easier explained in the case of uncoupled lattice.

In the uncoupled case the tunes (which are already known) can be expressed via the integrals of inverse β-functions. We can approximate the integrals by the sums (horizontal plane for instance)

$$Q_x = \frac{1}{2\pi}\oint \frac{ds}{\beta_x} \approx \frac{| a_{x0} |^2}{2\pi} \sum_{j=1}^{N_h} \frac{p_j}{| X_j(Q_x) |^2}, \tag{3.4}$$

where p_j are weight coefficients [$p_j = R(\theta_{j+1} - \theta_{j-1})/2$ by the trapezoid rule], and find the invariant amplitudes. Probably this method can be generalized on the case of coupled motion as well. However, it is not practical since: i) BPMs usually do not sample the ring sufficiently well, ii) the sum in eq.(3.4) is dominated by BPMs at low beta locations for which the signal to noise ratio is the lowest.

3.2 5-BPM algorithm

It is possible to circumvent the problem of determination of the invariant amplitudes if there is a region of the ring with known focusing properties. In such region β-functions can be found from the measured phase advances.

Since the focusing properties of the lattice assumed to be known we can calculate the transfer matrix between the BPMs, in particular its M_{12} and M_{34} elements which contain only β- and phase functions for the same plane, e.g.

$$M_{12}(\theta_j,\theta_l) = \sum_{m=1,2}\sqrt{\beta_{xm}(\theta_j)\beta_{xm}(\theta_l)}\,\sin[\varphi_{xm}(\theta_j)-\varphi_{xm}(\theta_l)] \tag{3.5}$$

For N_{BPM} in one plane we have $N_{\mathrm{BPM}}(N_{\mathrm{BPM}}-1)/2$ equations while the number of unknowns is $2\,N_{\mathrm{BPM}}$ (β_{x1} and β_{x2} or β_{y1} and β_{y2} at each BPM). Correspondingly, the minimum number of BPMs per plane needed is $N_{\mathrm{BPM}} = 5$. With β-functions at these 5 BPMs found we may use the first of eqs.(3.3) to evaluate the invariant amplitudes and then find β-functions in the rest of the ring.

This method requires data for both normal modes and is prone to errors, especially for the cross-plane functions.

4 PERTURBATION APPROACH

In practice there is always some ideal (design) optics which can be used as the first approximation. The goal of optics measurements is not only to find actual (perturbed) optics functions but also to detect the sources of perturbation and evaluate necessary changes in correction circuits. The problem may be complicated by BPM tilts and calibration errors. To unwind all these effects we have to resort to the method of successive approximations.

First of all let us establish relations between sources of perturbation and observable effects on beta-functions and phase advances assuming the perturbed motion to be stable (which requires the tunes to lie outside the stopbands of half-integer and sum resonances).

We may still use eq.(2.18) with the ideal eigenvectors but treat it now just as a linear transformation of variables [10]. Thus defined vector $\underline{a}$ is a linear superposition of the "true" normal forms $\underline{A}$:

$$\underline{a} = \mathrm{T}^{-1}(\theta)\underline{A} \tag{4.1}$$

(it is more convenient to define the direct transformation as $\underline{A} = \mathrm{T}\,\underline{a}$ in order to make the analysis presented in Appendix A simpler). Given the ideal optics functions and the transformation matrix T we can find the new eigenvectors matrix as

$$\mathrm{V}_{perturbed} = \mathrm{V}_{ideal}\,\mathrm{T}^{-1} \tag{4.2}$$

and, eventually, the perturbed lattice functions.

Appendix A describes a recipe (based on the Lie-transform theory) for finding T for a given perturbing Hamiltonian. Though our system is linear, the observable effects of perturbation (described by matrix T) are nonlinear in the perturbing element strength.

4.1 Uncoupled optics functions and BPM calibration

Let us first consider an uncoupled lattice. To determine the invariant amplitudes A_{m0} we can use the fact that the average value of the inverse β-function over many periods of betatron oscillations is not sensitive to beta-beating. Retaining in the sum only BPMs in regular sections (such as arcs) we get a rough estimate for the amplitude

$$|A_{x0}|^2 \approx \sum_j \frac{1}{\beta_{x0}(\theta_j)} \Big/ \sum_j \frac{1}{|X_j(Q_x)|^2} \tag{4.3}$$

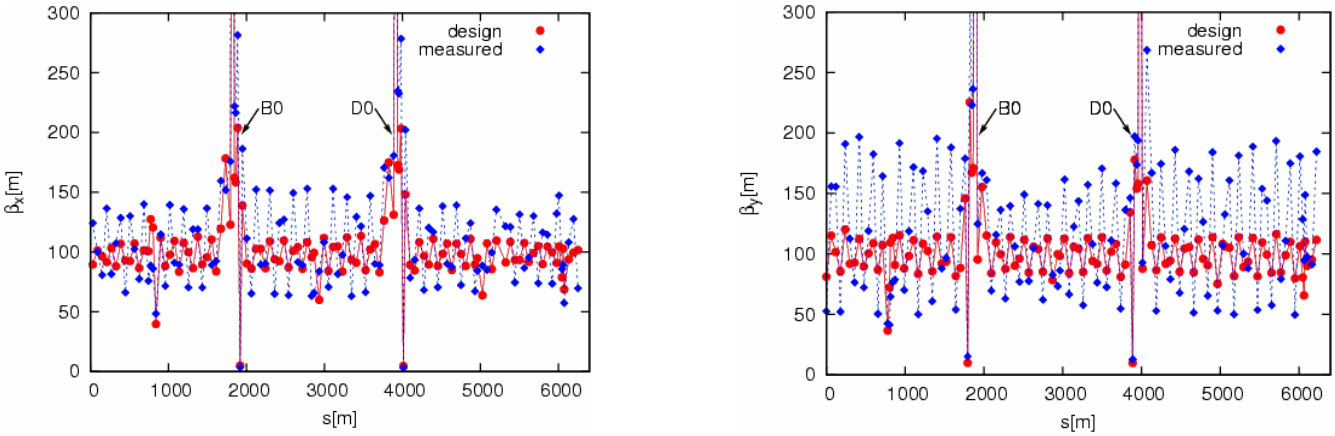

FIG. 1 (color). Measured and design Tevatron collision optics functions with tunes shifted to half-integer values vs. distance from F18 marker: left - β_x at horizontal BPMs, right - β_y at vertical BPMs

and, with the help of eqs.(3.3), for the optics functions.

Figure 1 presents thus found main beta-functions with the Tevatron collision optics as functions of the distance from F18 marker[2]. The tunes were intentionally shifted close to half-integer values $Q_x = 20.518$, $Q_y = 20.514$ which resulted in strong beta-beating.

Following the lead of section 3.2 it is possible to obtain a more precise estimate of the invariant amplitude provided there are regions free of large focusing perturbations. Now that the optics is uncoupled we need only 3 BPMs per plane to calculate the β-functions from the measured phase advances as was first noted by P. Castro-Garcia [13].

Taking the ideal transfer matrix between BPMs and measured phase advances we obtain equations for the product of β-functions [confer eq.(2.26)]:

$$\beta(\theta_j)\beta(\theta_k) = m_{jk}^2, \quad m_{jk} = |M_{12}(\theta_k, \theta_j)/\sin[\varphi(\theta_k) - \varphi(\theta_j)]|. \tag{4.4}$$

Applying this relation to pairs in a group of three BPMs we find the solution (provided the phase advance between any two of BPMs is not a multiple of π):

$$\begin{aligned} \beta^{(3)}(\theta_j) &= m_{jk} m_{jl} / m_{kl}, \\ \beta^{(2)}(\theta_k) &= m_{jk} m_{kl} / m_{jl}, \\ \beta^{(1)}(\theta_l) &= m_{kl} m_{jl} / m_{jk}. \end{aligned} \tag{4.5}$$

where superscripts denote BPM position in the group (from the right to the left).

This algorithm (which we will refer to as the 3-BPM algorithm) has in fact a greater potential: it permits to check if a particular region is really free of focusing perturbations and find BPM calibration errors.

Moving the 3-BPM window across a particular BPM we obtain three values, $\beta^{(n)}$, $n = 1, 2, 3$, for β-function at its location; the scatter in these values tells us whether this BPM belongs to a

[2] Locations in the Tevatron are labeled in the proton motion direction with a letter denoting the sector (A-F) and two numbers, the first one (0-4) being the "house" and the second one being the position in it. Interaction points are in the beginning of sectors B and D, the horizontal kicker used in TBT measurements is located at F17 which explains the choice of MF18 as the starting point in calculations.

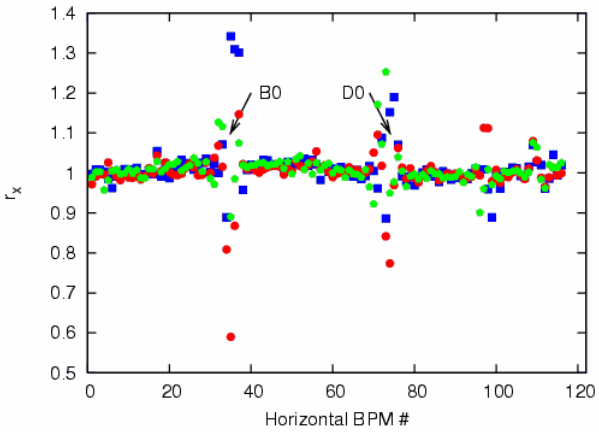

FIG. 2 (Color). Ratio of horizontal β-function values derived from phase advances to those inferred from amplitude of oscillations: blue squares - when the particular BPM is on the left side, green triangles – in the center, red circles – on the right side of the group. The count starts from F19 HBPM.

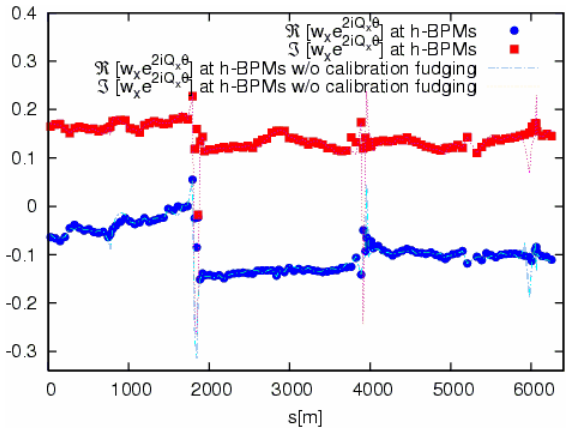

FIG. 3 (Color). Real and imaginary parts of function w_x describing horizontal beta-beating seen in Fig.1a with fudging of horizontal BPM calibration factors (blue triangles and red squares) and before fudging (dashed lines).

perturbation-free region. Fig. 2 shows the ratios of thus obtained values of the horizontal β-function to the approximate β_x values derived from amplitude of oscillations with the help of eqs.(3.3) and (4.3). One can see strong effect of focusing perturbations in the interaction regions and other straight sections.

In the perturbation-free regions where all three $\beta^{(n)}$ values for a given BPM are close to the average

$$\bar{\beta}(\theta_j) = \frac{1}{3}\sum_{n=1}^{3} \beta^{(n)}(\theta_j) \tag{4.6}$$

we may consider the ratio

$$r_j = \sqrt{\bar{\beta}_x(\theta_j) / \beta_x^{(app)}(\theta_j)}, \quad \beta_x^{(app)}(\theta_j) = | X_j(Q_x) / A_{x0} |^2, \tag{4.7}$$

as a relative calibration factor[3] (defined as $r = x_{\text{actual}} / x_{\text{reported}}$).

Now we can get a better estimate for the invariant amplitudes by requiring the average factors $\langle r \rangle$ over "good" BPMs to be equal to 1. In the considered example of the Tevatron collision optics these average values happened to be $\langle r_x \rangle$=1.014, $\langle r_y \rangle$=1.012 proving the validity of estimate (4.3) in the presence of strong beta-beating.

The 3-BPM algorithm fails in the regions containing sources of focusing perturbations, still we may try to separate the effects of focusing and calibration errors.

Let us develop the first of eqs.(3.2) using eq.(A.23) and introducing calibration factors:

$$\begin{aligned} & r_j X_j(Q_x) = (\mathrm{V}_{ideal}\mathrm{T}^{-1})_{11} e^{iQ_x\theta_j} A_{x0} = \\ & = \sqrt{\beta_{x0}^{(j)}} \, (e^{i\phi_{x0}^{(j)} + iQ_x\theta_j} \underbrace{\cosh u_x \cdot A_{x0}}_{C_j} + e^{-i\phi_{x0}^{(j)} - iQ_x\theta_j} \underbrace{e^{i\arg w_x + 2iQ_x\theta_j} \sinh u_x \cdot A_{x0}}_{S_j}), \end{aligned} \tag{4.8}$$

[3] It should be noted that by using only TBT information it is not possible to determine absolute calibration factors.

our goal being to find function w_x [relation of its absolute value to u_x is given in eq.(A.23)] and calibration errors.

Usually there are only few elements with strong focusing errors, let us assume that between two adjacent BPMs (say, j-th and $(j+1)$-th) there is no such elements. Then according to eq.(A.20) C_j, S_j have constant values at these BPMs which can be found as functions of calibration factors r_j, r_{j+1}.

Thus determined C_j, S_j (index j denotes the interval between j-th and $(j+1)$-th BPMs) may oscillate strongly from one interval to another. By fudging the calibration factors functions C_j, S_j can be made to vary more smoothly over a chosen range even if it includes perturbing elements.

Figure 3 shows function $\exp(2iQ_x\theta)\cdot w_x(\theta)$ calculated with all BPM calibration factors set to 1 (dashed lines) and with calibration factors found with either the 3-BPM algorithm (in perturbation-free regions) or the described above fudging procedure (triangles and squares). The largest calibration errors were found for B0 collision point monitors (HB0U and HB0D): $r_{34} = 0.964$, $r_{35} = 1.055$, and for HD12 monitor downstream of D0: $r_{76} = 1.075$. It can be seen that the fudging reduces oscillations in $|w_x|$ while preserving its abrupt changes indicating the position of perturbing elements.

4.2 Coupled optics functions

For simplicity we assume the ideal lattice to be uncoupled and consider coupling as a perturbation.

Let us work out eqs.(3.2) using transformation matrix (A.37) and allowing for BPM tilts. If the first normal mode was excited we have for the Fourier components of the TBT beam positions

$$\begin{aligned} X_j(Q_1) &= \sqrt{\beta_{x0}}\,(e^{i\phi_{x0}} + e^{-i\phi_{x0}}\sec\kappa\, u_x)\cos\kappa\, A_{10}e^{iQ_1\theta_j}, \\ Y_l(Q_1) &= [\sqrt{\beta_{y0}}\,\frac{\tan\kappa}{\kappa}(e^{-i\phi_{y0}}u_+ - e^{i\phi_{y0}}u_-) - \sqrt{\beta_{x0}}e^{i\phi_{x0}}\sin\chi_l]\cos\kappa\, A_{10}e^{iQ_1\theta_l}, \end{aligned} \tag{4.9}$$

where $\kappa = \sqrt{|u_-|^2 - |u_+|^2}$, function u_x includes effect of focusing errors (see section A.2) as well as second-order coupling effect ($w_{2x}/2$) given by eq.(A.34). BPM tilt angle χ is considered positive for tilt from x to y.

If the second mode was excited we analogously have

$$\begin{aligned} Y_l(Q_2) &= \sqrt{\beta_{y0}}\,(e^{i\phi_{y0}} + e^{-i\phi_{y0}}\sec\kappa\, u_y)\cos\kappa\, A_{20}e^{iQ_2\theta_l}, \\ X_j(Q_2) &= [\sqrt{\beta_{x0}}\,\frac{\tan\kappa}{\kappa}(e^{-i\phi_{x0}}u_+ + e^{i\phi_{x0}}u_-^*) + \sqrt{\beta_{y0}}e^{i\phi_{y0}}\sin\chi_j]\cos\kappa\, A_{20}e^{iQ_2\theta_j}. \end{aligned} \tag{4.10}$$

Before discussing the algorithm for finding $u_\pm$ let us note that in eqs. (4.9), (4.10) we neglected higher order terms in $u_{x,y}$ but retained those in $u_\pm$ (represented by κ). Higher order terms in $u_\pm$ may be significant only when the tunes are close to a coupling resonance (sum and/or difference), but then these functions are nearly constant around the ring by the absolute value. Therefore κ can always be assumed constant.

Again, the first step is to find the invariant amplitudes A_{m0}. To get rid of the effect of beta-beating we can use eq.(4.3) and obtain an estimate for $\cos\kappa\cdot A_{m0}$. Dividing by this product eqs.(4.9) or eqs.(4.10) (depending on which mode has been excited) we get for each BPM in the orthogonal plane just one equation for two unknowns: $z_\pm = u_\pm \tan\kappa/\kappa$. Therefore some additional relation is necessary.

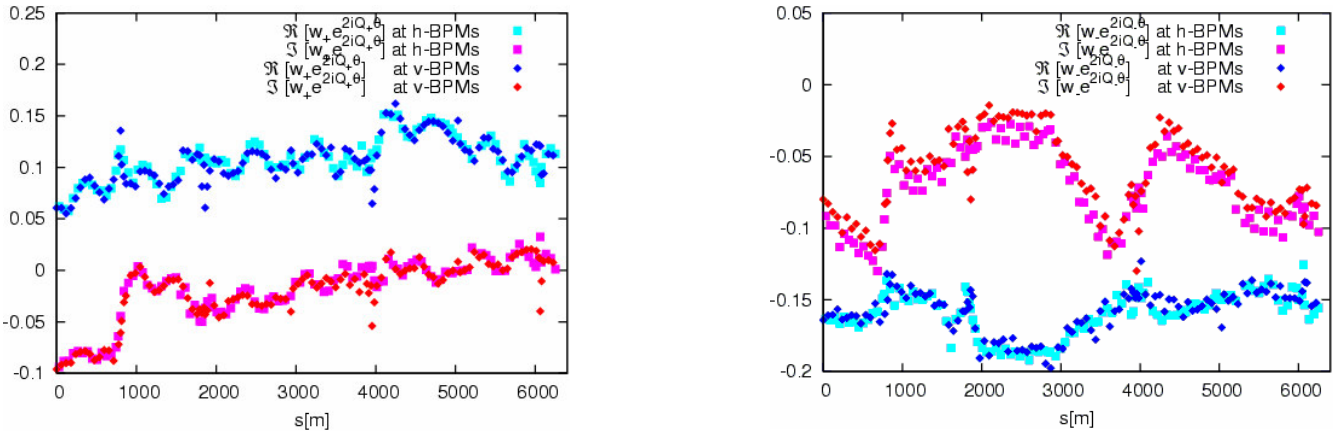

FIG. 4 (Color). Real and imaginary parts of functions w_+ (left) and w_- (right) describing linear coupling found from the first (horizontal) mode seen in the vertical BPMs (blue and red) and the second mode seen in the horizontal BPMs (cyan and magenta) in the case of the Tevatron collision optics.

As shown in section A.4, in regions free of couplers the first-order generating functions behave as $w_\pm(\theta) = \text{const} \times \exp[-i(Q_{x0} \pm Q_{y0})\theta]$. Assuming such dependence for $z_\pm$ in the interval between two BPMs of the same orientation[4] we get two additional equations allowing to find $z_\pm$ at these BPMs and in the interval between them. Inverting the definition of $z_\pm$ and using eq.(A.38) we obtain the first-order generating functions

$$w_\pm = z_\pm (1 \mp |z_\pm|^2 \pm |z_\mp|^2 / 3) \tag{4.11}$$

Figure 4 presents functions $\exp[i(Q_x \pm Q_y)\theta] \cdot w_\pm(\theta)$ found from the first (horizontal) mode seen in the vertical BPMs and the second (vertical) mode in the horizontal BPMs in the case of the Tevatron collision optics at nominal tunes $Q_x = 20.585$, $Q_y = 20.575$. Good agreement of the two sets of values demonstrates reliability of the method.

By differentiating the generating functions we can find the distribution functions of couplers defined in eq.(A.27):

$$C_\pm(\theta) = 2ie^{-iQ_{0\pm}\theta} \frac{d}{d\theta} e^{iQ_{0\pm}\theta} w_\pm(\theta), \tag{4.12}$$

where $Q_{0\pm} = Q_{x0} \pm Q_{y0}$. Jumps in $w_\pm$ correspond to the presence of strong couplers. The largest jump in Figs. 4 occurs at approximately 800m from the origin and corresponds to two SQA0 skew quadrupoles used for coupling compensation. Another jump happens downstream of D0 at about 4100m and was traced to a tilt of D16 defocusing quadrupole.

The knowledge of $C_\pm$, $w_\pm$ (and κ) permits to calculate the second order functions $w_{2x,y}$ [see eqs.(A.34)] and separate the effects of focusing errors and coupling on beta-beating. Figure 5 shows the absolute values of functions $w_{x,y}$ as determined from data (and presented in Fig.3 for the horizontal plane) and with the coupling contribution subtracted. One can see that the coupling contribution reaches 20% and in its absence the amplitude of beta-beating would have been approximately equal in both planes.

[4] It is easy to see that two BPMs of different orientation (one horizontal and one vertical) can not be used even when data for both normal modes is available since (after z_+ exclusion) the resulting equation, $\exp(2i\phi_{y0})\, z_- + \exp(2i\phi_{x0})\, z_-^* = \text{r.h.s.}$, has zero determinant.

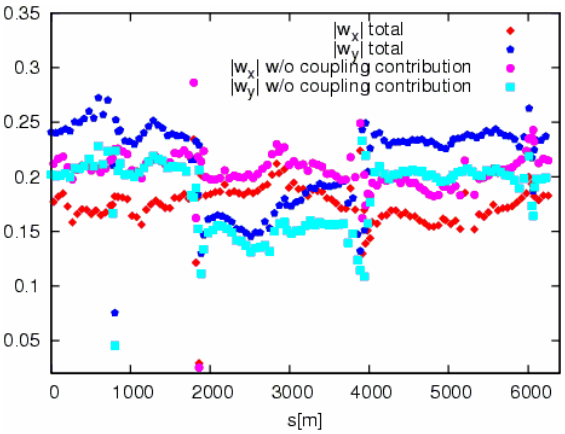

FIG. 5 (Color). Absolute values of functions $w_{x,y}$ as determined from data with (red and blue) and without (magenta and cyan) the coupling contribution.

4.3 Global coupling coefficients

Let $n_\pm$ be the closest integers to the sum and difference of the tunes, $n_\pm = \mathrm{Round}(Q_x \pm Q_y)$. The resonance driving terms (which can also be called the global coupling coefficients) are the corresponding Fourier harmonics of the couplers distribution:

$$c_\pm \equiv \frac{1}{2\pi}\int_0^{2\pi} e^{in_\pm\theta} C_\pm d\theta\,. \tag{4.13}$$

Of these two values c_- bears more practical importance since its absolute value determines the closest tune approach (see Appendix D). Substitution of eq.(4.12) into eq.(4.13) gives the relation between the coupling coefficients and generating functions:

$$c_\pm = -\frac{Q_{0\pm} - n_\pm}{\pi}\int_0^{2\pi} e^{in_\pm\theta} w_\pm d\theta = -2(Q_{0\pm} - n_\pm) w_\pm^{(-n_\pm)}. \tag{4.14}$$

This relation requires TBT data acquisition from all BPMs around the ring which may be too lengthy a process for practical application of this method.

The solution follows from the observation made in Appendix A [see eq.(A.31)] that close to the resonance $Q_x \pm Q_y = n_\pm$ the corresponding generating function is dominated by the resonance harmonic, $w_\pm(\theta) \approx \mathrm{const} \times \exp(-in_\pm\theta)$, so that any part of the ring is representative of the whole. Working close to a resonance also reduces error due to BPM tilts. However, there is a minor complications since the tunes which enter eq.(4.14) are not directly measured tunes but the would-have-been tunes in the absence of coupling.

The exact relation between the ideal and perturbed tunes in the near-resonance case is given in Appendix D. For practical purposes we can limit ourselves to the second order correction in the coupling strength to obtain

$$c_\pm \approx -2\frac{Q_\pm - n_\pm}{\sqrt{1 \mp 4\,|\,w_\pm\,|^2}} w_\pm^{(-n_\pm)} \approx -\frac{2(Q_\pm - n_\pm)\,\bar{z}_\pm}{1 \mp |\,\bar{z}_\pm\,|^2 \mp |\,\bar{z}_\mp\,|^2\,/3}, \tag{4.15}$$

where $Q_\pm = Q_x \pm Q_y$ are combinations of the measured tunes, the bar means averaging with exponential $\exp(in_\pm\theta)$ over the available range:

$$\bar{z}_\pm = \frac{1}{\theta_2 - \theta_1}\int_{\theta_1}^{\theta_2} e^{in_\pm\theta} z_\pm d\theta\,. \tag{4.16}$$

4.4 BPM tilts

When finding generating functions $w_\pm$ from eqs.(4.9) or eqs.(4.10) we assumed the BPM tilts to be known. In the interval between two BPMs functions $w_\pm$ depend on tilts of only these two BPMs. If one of the BPMs has large unaccounted tilt it will produce strong oscillations of functions $w_\pm$ in the adjacent intervals. By fudging the tilt angles χ_j, functions $w_\pm$ can be made to vary smoothly over a chosen range even if it includes strong couplers. Such a procedure had already been applied to

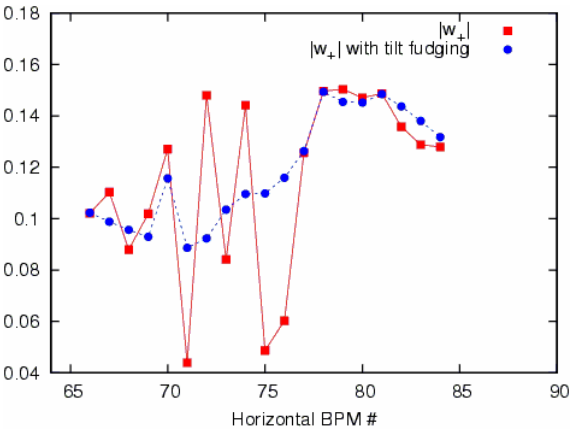

FIG. 6 (Color). Absolute value of function w+ determined from the second mode seen in the horizontal BPMs in the region C36-D28 before (red) and after (blue) fudging of BPM tilts.

functions shown in Fig. 4 in interaction regions and some of straight sections. Figure 6 demonstrates the effect of fudging of the horizontal BPM tilt on w_+ in the interval which includes D0 interaction region. The largest angle of +4° was found for HC44 monitor.

Let us note that a systematic tilt of BPMs in arc cells with equal phase advance in both planes introduces systematic error in the difference resonance generating function of magnitude

$$|\delta w_-| \approx \sqrt{\frac{1-\sin\mu/2}{1+\sin\mu/2}}\sin\chi \qquad (4.17)$$

where μ is the betatron phase advance per cell. In the Tevatron $\mu \approx 2\pi/5$ and systematic tilt by 1° would produce an error $|\delta w_-| \approx 0.009$. With $Q_- = .01$ the resulting error in coupling coefficient is fairly small:

$|\delta c_-| \approx 0.0002$.

ACKNOWLEDGEMENTS

The authors are grateful to V.Lebedev and L.Michelotti for many helpful remarks.

APPENDIX A. LIE-TRANSFORM PERTURBATION THEORY

In the presence of perturbations we may use eq.(2.18) with the ideal matrix V just as a linear transformation of variables. Let us make an important remark here. By making the eigenvectors periodic with the help of the exponential factor in eq.(2.13) we ensured the periodicity in θ of the transformed Hamiltonian $\mathcal{U}$ and will impose the periodicity condition on all lattice functions that will appear in the following – e.g. new Hamiltonian $\mathcal{K}$, generating function $\mathcal{W}$ – not always mentioning it.

Now let us rewrite the Hamiltonian $\mathcal{U}$ introducing the perturbation parameter ε

$$\mathcal{U}(\underline{a}, \theta; \varepsilon) = \mathcal{U}_0(\underline{a}) + \varepsilon\mathcal{U}_1(\underline{a}, \theta) \qquad (A.1)$$

where $\mathcal{U}_0$ is given by eq.(2.22) with the ideal tunes, Q_{10}, Q_{20}, and $\mathcal{U}_1$ is given by eq.(2.24) with $\mu = 2$. Parameter ε, introduced for later convenience, varies from ε=0 for the ideal lattice to ε=1 for the real lattice.

Since we assume our system still to be linear (and stable), there should be "true" normal forms, $\underline{A}$; our goal is to find their relation to the original dynamic variables, $\underline{a}$.

By saying that the new variables $\underline{A}$ are "true" normal forms we mean that Hamiltonian, $\mathcal{K}$, which governs motion in these variables,

$$\frac{d}{d\theta}\underline{A} = \mathrm{S}\frac{\partial}{\partial \underline{A}}\mathcal{K}, \qquad (A.2)$$

is of the type (2.22) with new (perturbed) tunes Q_1, Q_2.

Vector $\underline{A}$ is a linear combination of the original variables with coefficients depending on parameters ε and θ:

$$\underline{A} = \mathrm{T}(\varepsilon, \theta)\underline{a} \tag{A.3}$$

It satisfies the boundary condition $\underline{A}\,|_{\varepsilon\to 0} = \underline{a}$, or, for the transformation matrix T:

$$\mathrm{T}\,|_{\varepsilon\to 0} = \mathrm{I}, \tag{A.4}$$

I being the identity matrix. It is obvious that $\mathcal{K}\,|_{\varepsilon\to 0} = \mathcal{U}_0$.

By properly scaling variables $\underline{A}$ with ε we can ensure matrix T being unimodular (and therefore symplectic since $\underline{A}$ is in normal form for all values of ε); the knowledge of T enables us to find the matrix of new eigenvectors $\mathrm{V}_{perturbed}=\mathrm{V}_{ideal}\mathrm{T}^{-1}$ and, eventually, the perturbed lattice functions.

In the linear case under consideration, the Hamiltonians (both original and new) are bilinear forms:

$$\mathcal{U} = \frac{1}{2}\underline{a}^T\,\mathrm{U}\,\underline{a}, \quad \mathcal{K} = \frac{1}{2}\underline{A}^T\,\mathrm{K}\,\underline{A}, \tag{A.5}$$

with symmetric matrices $\mathrm{U}^T=\mathrm{U}$, $\mathrm{K}^T=\mathrm{K}$. Making notice that

$$\begin{aligned}\frac{d}{d\theta}\underline{A} &= \frac{\partial \mathrm{T}}{\partial\theta}\underline{a} + \mathrm{TS}\,\mathrm{U}\,\underline{a} = (\frac{\partial \mathrm{T}}{\partial\theta} + \mathrm{TSU})\,\mathrm{T}^{-1}\,\underline{A} \\ &= \mathrm{SK}\,\underline{A}\end{aligned}$$

we get an equation linking T and K:

$$\frac{\partial \mathrm{T}}{\partial\theta} = \mathrm{SKT} - \mathrm{TS}\,\mathrm{U} \tag{A.6}$$

Despite its apparent simplicity, eq.(A.6) is not convenient to use since it does not incorporate the condition of matrix T symplecticity. To do this we may recall the powerful Lie-transform perturbation theory [11]. Specifically, we may consider the transition from the ideal to the perturbed system as a "motion" governed by some Hamiltonian, $\mathcal{W}$, with the perturbation parameter ε playing the role of time:

$$\frac{d}{d\varepsilon}\underline{A} = \mathrm{S}\frac{\partial}{\partial\underline{A}}\mathcal{W} = \mathrm{SW}\,\underline{A}, \tag{A.7}$$

where W is the (symmetric) matrix of bilinear form $\mathcal{W}$: $\mathcal{W} = \underline{A}^T\mathrm{W}\underline{A}\,/2$. Then the transformation matrix T will be symplectic by construction. Substituting eq.(A.3) into eq.(A.7) we obtain an equation for its evolution with "time" ε:

$$\frac{\partial \mathrm{T}}{\partial\varepsilon} = \mathrm{S}\,\mathrm{WT} \tag{A.8}$$

Now, equating mixed derivatives of T obtained from eqs.(A.6), (A.8) we arrive at the matrix analogue of Dewar's equation (see e.g. Ref.[14])

$$\frac{\partial \mathrm{W}}{\partial\theta} + \mathrm{WSK} - \mathrm{KSW} = \frac{\partial \mathrm{K}}{\partial\varepsilon} - (\mathrm{T}^{-1})^T\,\frac{\partial \mathrm{U}}{\partial\varepsilon}\mathrm{T}^{-1} \tag{A.9}$$

Expansion of this equation in powers of ε leads to the matrix analogue of the Deprit equations. But let us first note that if matrix $\mathrm{SW}(\varepsilon)$ is self-commutative at different values of ε, i.e. if $\mathrm{W}(\varepsilon_1)\mathrm{SW}(\varepsilon_2) = \mathrm{W}(\varepsilon_2)\mathrm{SW}(\varepsilon_1)$, then

$$\mathrm{T}(\varepsilon) = \exp[\mathrm{S}\int_0^{\varepsilon} \mathrm{W}(\varepsilon')d\varepsilon'] . \tag{A.10}$$

A.1 Power expansion

Generally we have to resort to power expansion in ε:

$$\begin{aligned} &\mathrm{U} = \sum_{n=0}^{\infty} \frac{\varepsilon^n}{n!} \mathrm{U}_n, \quad \mathrm{K} = \sum_{n=0}^{\infty} \frac{\varepsilon^n}{n!} \mathrm{K}_n, \quad \mathrm{K}_0 = \mathrm{U}_0, \\ &\mathrm{W} = \sum_{n=0}^{\infty} \frac{\varepsilon^n}{n!} \mathrm{W}_{n+1}, \quad \mathrm{T} = \sum_{n=0}^{\infty} \frac{\varepsilon^n}{n!} \mathrm{T}_n, \quad \mathrm{T}_0 = \mathrm{I}. \end{aligned} \tag{A.11}$$

From eq.(A.8) and the identity TT^{-1}=I we immediately get the recursion relations

$$\begin{aligned} &\mathrm{T}_{n+1} = \mathrm{S} \sum_{k=0}^{n} \frac{n!}{k!(n-k)!} \mathrm{W}_{n-k+1} \mathrm{T}_k , \\ &(\mathrm{T}^{-1})_{n+1} = -\sum_{k=0}^{n} \frac{n!}{k!(n-k)!} (\mathrm{T}^{-1})_k \, \mathrm{SW}_{n-k+1} \end{aligned} \tag{A.12}$$

Substitution of ansatz (A.11) into eq.(A.9) leads to a chain of matrix analogues of the Deprit equations (see e.g. Ref.[11]). Here we will not give the general formula but limit ourselves to the first three of these equations:

$$\begin{aligned} &\hat{D}\,\mathrm{W}_1 = \mathrm{K}_1 - \mathrm{U}_1, \\ &\hat{D}\,\mathrm{W}_2 = \mathrm{K}_2 - \mathrm{U}_2 - (\mathrm{W}_1, \mathrm{K}_1 + \mathrm{U}_1), \\ &\hat{D}\,\mathrm{W}_3 = \mathrm{K}_3 - \mathrm{U}_3 - (\mathrm{W}_1, \mathrm{K}_2 + 2\,\mathrm{U}_2) - (\mathrm{W}_2, 2\,\mathrm{K}_1 + \mathrm{U}_1) - (\mathrm{W}_1, (\mathrm{W}_1, \mathrm{U}_1)), \end{aligned} \tag{A.13}$$

where the binary matrix operation (A, B)=ASB-BSA and operator $\hat{D}$, $\hat{D}\,\mathrm{W} \equiv \partial_\theta \mathrm{W} + (\mathrm{W}, \mathrm{K}_0)$, were introduced.

To achieve our goal - find transformation T which brings Hamiltonian $\mathcal{K}$ to the form (2.22) - the matrices W_n should absorb the offending terms from the r.h.s. of eqs.(A.13). There can be terms which are not in the range of operator $\hat{D}$, such terms have to be relegated to K_n. Since we excluded the resonance case from consideration these only can be the tuneshift terms.

A.2 Focusing perturbations

Let us consider an uncoupled lattice and present formulas for only one plane (say, horizontal). The matrix of the ideal Hamiltonian is

$$\mathrm{K}_0 = \mathrm{U}_0 = \begin{pmatrix} 0 & iQ_0 \\ iQ_0 & 0 \end{pmatrix} \tag{A.14}$$

Now let us introduce quadrupole field errors with gradient

$$k_1 = \frac{1}{B\rho} \frac{\partial}{\partial x} \delta B_y \tag{A.15}$$

We have for the perturbing Hamiltonian (the sign of k_1 should be reversed for the vertical plane):

$$\mathcal{U}_1 = \frac{i}{4} R k_1 x^2 = \frac{i}{2} R k_1 \beta_0 a a^* + \frac{i}{4} R k_1 \beta_0 (e^{2i\phi_0} a^2 + e^{-2i\phi_0} a^{*2}), \tag{A.16}$$

The mean value over the machine circumference of the first term in the r.h.s. of eq.(A.16) (more precisely, of its matrix) is not in the range of operator $\hat{D}$ and therefore constitutes $\mathcal{K}_1$:

$$\mathcal{K}_1 = \frac{i}{4\pi} \int_0^{2\pi R} k_1 \beta_0 ds \; a a^* \;\Rightarrow\; \delta Q = \frac{1}{4\pi} \int_0^{2\pi R} k_1 \beta_0 ds \,, \tag{A.17}$$

the leftover being absorbed by $\mathcal{W}_1$. Since the effect of the first term can not be resonantly enhanced we will ignore it altogether and instead focus on the last two terms in the r.h.s. of eq.(A.16) presented by matrix

$$\mathrm{U}_1 = \begin{pmatrix} ige^{2i\phi_0} & 0 \\ 0 & ige^{-2i\phi_0} \end{pmatrix}, \quad g = \frac{1}{2} R k_1 \beta_0 . \tag{A.18}$$

This matrix is well within the range of operator $\hat{D}$ so it does not contribute to K_1. Since we have neglected the contribution from the first term we have K_1=0. Together with the periodicity condition, $\mathrm{W}_1(2\pi)= \mathrm{W}_1(0)$, the first of eqs.(A.13) yields solution for W_1:

$$\mathrm{W}_1 = \begin{pmatrix} w & 0 \\ 0 & -w^* \end{pmatrix}, \quad w(\theta) = -\int_0^{2\pi} \frac{e^{-2iQ_0[\theta - \pi \,\mathrm{sign}(\theta-\theta')] + 2i\varphi_0(\theta')}}{2 \sin 2\pi Q_0} g(\theta') d\theta' . \tag{A.19}$$

(we recalled definition $\phi = \varphi - Q\theta$).

It is easy to see that in perturbation-free regions

$$w(\theta) = \text{const} \times \exp(-2iQ_0\theta), \tag{A.20}$$

whereas at localized sources of quadrupole errors function $w(\theta)$ exhibits a discontinuity:

$$\Delta w = -ige^{2i\phi_0} \Delta\theta = -\frac{i}{2} k_1 L \beta_0 e^{2i\phi_0} , \tag{A.21}$$

where L is the source length. This fact can be used for identification of perturbing elements.

A.2.1 Near-resonance case

If the tune is close to an integer or a half integer the resonance harmonics $n = Integer(2Q_0)$ dominates $w(\theta)$:

$$w(\theta) \approx \frac{g_{-n} e^{-in\theta}}{n - 2Q_0}, \quad g_{-n} = \frac{1}{2\pi} \int_0^{2\pi} e^{i(n-2Q_0)\theta + 2i\varphi_0(\theta)} g(\theta) d\theta \tag{A.22}$$

so that $w(\theta)$ is about constant around the ring by the absolute value.

Since the effect of the focusing perturbations is resonantly enhanced the higher order terms in the W expansion may become important. Dominance of one (resonance) harmonic in W makes eq.(A.10) applicable leading to the result:

$$\mathrm{T}^{-1} \approx \begin{pmatrix} \cosh u & e^{-i\arg w}\sinh u \\ e^{i\arg w}\sinh u & \cosh u \end{pmatrix}, \quad u = \frac{1}{2}\,\mathrm{Arc}\tanh 2\,|\,w\,|\,. \tag{A.23}$$

It is exact when $g(\theta)$ contains only one harmonic from the beginning. Of course, there is a well-known exact expression for the tune in this case as well: $(Q - n/2)^2 = (Q_0 - n/2)^2 - |g_{-n}|^2$.

Presenting the new eigenvectors (columns of matrix $\mathrm{V}_{perturbed}=\mathrm{V}_{ideal}\mathrm{T}^{-1}$) in the form (2.25) we obtain for the perturbed lattice functions:

$$\begin{aligned} \frac{\beta}{\beta_0} &= \cosh 2u + \sinh 2u\,\cos(2\phi_0 - \arg w) = \frac{1 + 2\,|\,w\,|\cos(2\phi_0 - \arg w)}{\sqrt{1 - 4\,|\,w\,|^2}}, \\ \phi &= \phi_0 - \arctan\frac{\tanh u\,\sin(2\phi_0 - \arg w)}{1 + \tanh u\,\cos(2\phi_0 - \arg w)}. \end{aligned} \tag{A.24}$$

Recalling that in perturbation-free regions $\arg w = -2Q_0\theta + const$ we retrieve the well-known fact that the beta-wave propagates at twice the betatron phase advance: $2\phi_0 - \arg w = 2\varphi_0 - const$.

The beta wave of relative amplitude $b = \Delta\beta/\beta_0$ (= $\sinh 2u$) increases the average value of β-function over the beating period as

$$< \beta/\beta_0 >= \sqrt{1 + b^2} \tag{A.25}$$

However, the average value of the *inverse* β-function, $<\beta_0/\beta>$, in the considered approximation does not deviate from 1 by more than the relative tuneshift.

A.3 Coupling perturbations

In this case the matrix of the perturbing Hamiltonian is:

$$\mathrm{U}_1 = \frac{i}{2}\begin{pmatrix} 0 & 0 & C_+ & C_- \\ 0 & 0 & C_-^* & C_+^* \\ C_+ & C_-^* & 0 & 0 \\ C_- & C_+^* & 0 & 0 \end{pmatrix} \tag{A.26}$$

with

$$C_\pm(\theta) = \frac{R\sqrt{\beta_x\beta_y}}{2B\rho}\left\{\left(\frac{\partial B_x}{\partial x} - \frac{\partial B_y}{\partial y}\right) + B_\theta\left[\left(\frac{\alpha_x}{\beta_x} - \frac{\alpha_y}{\beta_y}\right) - i\left(\frac{1}{\beta_x} \mp \frac{1}{\beta_y}\right)\right]\right\} e^{i(\phi_x \pm \phi_y)} \tag{A.27}$$

being driving terms of linear sum and difference resonances; $\mathrm{U}_n = 0$ for $n \geq 2$. U_1 is in the range of operator $\hat{D}$, correspondingly $\mathrm{K}_1 = 0$.

The matrix of the first-order generating function is easily found from eq.(A.13) to be

$$\mathrm{W}_1 = \begin{pmatrix} 0 & 0 & w_+ & w_- \\ 0 & 0 & -w_-^* & -w_+^* \\ w_+ & -w_-^* & 0 & 0 \\ w_- & -w_+^* & 0 & 0 \end{pmatrix}, \tag{A.28}$$

with

$$w_{\pm}(\theta) = -\int_0^{2\pi} \frac{\exp\{-i(Q_x \pm Q_y)[\theta - \theta' - \pi\,\mathrm{sgn}(\theta - \theta')]\}}{4\sin\pi(Q_x \pm Q_y)} C_{\pm}(\theta')d\theta'. \qquad (A.29)$$

In perturbation-free regions these functions are constant by absolute value: $w_{\pm}(\theta) = const \times \exp[-i(Q_x \pm Q_y)\theta]$; at a localized coupling source they exhibit a discontinuity:

$$\Delta w_{\pm} = -\frac{iC_{\pm}L}{2R} \qquad (A.30)$$

where L is the coupler length. This fact can be used for location of strong couplers.

When the tunes are close to either of the linear coupling resonances, $\Delta_{\pm} = Q_x \pm Q_y - n_{\pm} \approx 0$, the corresponding function (w_+ or w_-) is dominated by the resonance harmonic

$$w_{\pm} \approx -\frac{1}{2\Delta_{\pm}} c_{\pm} e^{-in_{\pm}\theta}, \qquad c_{\pm} \equiv \frac{1}{2\pi}\int_0^{2\pi} e^{in_{\pm}\theta} C_{\pm} d\theta \qquad (A.31)$$

and is about constant around the ring by the absolute value.

A.3.1 Higher order effects

When $|w_{\pm}|$ is not small compared to unity (due to either strength of coupling or closeness to a resonance) the higher order effects may become important. Let us have a look at the second and third order generating functions W_2, W_3.

Contribution from W_1 to the r.h.s. of the equation for W_2 is

$$(\mathrm{W}_1, \mathrm{U}_1) = \begin{pmatrix} i(-C_+w_- + C_-w_+) & i\,\mathrm{Re}(C_+w_+^* - C_-w_-^*) & 0 & 0 \\ i\,\mathrm{Re}(C_+w_+^* - C_-w_-^*) & i(-C_+^*w_-^* + C_-^*w_+^*) & 0 & 0 \\ 0 & 0 & i(C_+w_-^* + C_-^*w_+) & i\,\mathrm{Re}(C_+w_+^* + C_-w_-^*) \\ 0 & 0 & i\,\mathrm{Re}(C_+w_+^* + C_-w_-^*) & i(C_+^*w_- + C_-w_+^*) \end{pmatrix}. \qquad (A.32)$$

The off-diagonal elements of the diagonal blocks render (upon averaging) the second-order tuneshifts:

$$\Delta Q_x = \frac{1}{2\pi}\mathrm{Re}\int_0^{2\pi}(C_+w_+^* - C_-w_-^*)d\theta, \quad \Delta Q_y = \frac{1}{2\pi}\mathrm{Re}\int_0^{2\pi}(C_+w_+^* + C_-w_-^*)d\theta, \qquad (A.33)$$

whereas the diagonal elements are responsible for the beta-beating which can be described by diagonal blocks in W_2 of type (A.19) with

$$\begin{aligned} w_{2x}(\theta) &= \int_0^{2\pi} \frac{e^{-2iQ_{x0}[\theta-\theta'-\pi\,\mathrm{sign}(\theta-\theta')]}}{2\sin 2\pi Q_{x0}}(C_+w_- - C_-w_+)d\theta', \\ w_{2y}(\theta) &= -\int_0^{2\pi} \frac{e^{-2iQ_{y0}[\theta-\theta'-\pi\,\mathrm{sign}(\theta-\theta')]}}{2\sin 2\pi Q_{y0}}(C_+w_-^* + C_-^*w_+)d\theta', \end{aligned} \qquad (A.34)$$

For the second-order beta-beating to be noticeable the tunes should be close to the crossing point of linear resonances: two one-dimensional half-integer resonances and two coupling resonances (sum and difference). Such working points are often used in colliders since they minimize the beam-beam tuneshifts.

If the working point is not close to both coupling resonances simultaneously we may neglect the contribution from W_2 to higher order terms (but keep itself). Introducing matrix

$$\mathrm{F} = \int_0^1 \mathrm{W}(\varepsilon) d\varepsilon \approx \mathrm{W}_1 + \frac{1}{2}\mathrm{W}_2 + \frac{1}{6}\mathrm{W}_3, \tag{A.36}$$

and ignoring the dependence of $|w_{\pm}|$ on θ we obtain

$$\mathrm{T}^{-1} \approx e^{-\mathrm{SF}} \approx \begin{pmatrix} \cos\kappa & w_{2x}^*/2 & u_-^* \sin\kappa/\kappa & u_+^* \sin\kappa/\kappa \\ w_{2x}/2 & \cos\kappa & u_+ \sin\kappa/\kappa & u_- \sin\kappa/\kappa \\ -u_- \sin\kappa/\kappa & u_+^* \sin\kappa/\kappa & \cos\kappa & w_{2y}^*/2 \\ u_+ \sin\kappa/\kappa & -u_-^* \sin\kappa/\kappa & w_{2y}/2 & \cos\kappa \end{pmatrix}, \tag{A.37}$$

where

$$\begin{aligned} &\kappa = \sqrt{|u_-|^2 - |u_+|^2}, \\ &u_{\pm} \approx w_{\pm}\,[1 \pm \frac{2}{3}(2|w_{\pm}|^2 - |w_{\mp}|^2)]. \end{aligned} \tag{A.38}$$

Writing the new eigenvectors (columns of matrix $\mathrm{V}_{perturbed}=\mathrm{V}_{ideal}\mathrm{T}^{-1}$) in the form (2.21) we obtain for the perturbed lattice functions (ideal lattice is assumed to be uncoupled):

$$\begin{aligned} &\beta_{x1} = \beta_{x0}\,|\cos\kappa + \frac{1}{2}e^{-2i\phi_{x0}} w_{2x}|^2, \quad \phi_{x1} = \phi_{x0} + \arg(\cos\kappa + \frac{1}{2}e^{-2i\phi_{x0}} w_{2x}), \\ &\beta_{y2} = \beta_{y0}\,|\cos\kappa + \frac{1}{2}e^{-2i\phi_{y0}} w_{2y}|^2, \quad \phi_{y2} = \phi_{y0} + \arg(\cos\kappa + \frac{1}{2}e^{-2i\phi_{y0}} w_{2y}), \\ &\beta_{y1} = \beta_{y0}\frac{\sin^2\kappa}{\kappa^2}|e^{i\phi_{y0}}u_- - e^{-i\phi_{y0}}u_+^*|^2, \ \phi_{y1} = \arg(-e^{i\phi_{y0}}u_- + e^{-i\phi_{y0}}u_+^*), \\ &\beta_{x2} = \beta_{x0}\frac{\sin^2\kappa}{\kappa^2}|e^{i\phi_{x0}}u_-^* + e^{-i\phi_{x0}}u_+|^2, \ \phi_{x2} = \arg(e^{i\phi_{x0}}u_-^* + e^{-i\phi_{x0}}u_+), \end{aligned} \tag{A.39}$$

For function ω we have in the considered approximation

$$\omega = \sin^2\kappa. \tag{A.40}$$

Comparing with eq.(2.23) we obtain for Edwards-Teng's "symplectic rotation" angle $\Phi = \kappa$. We see that this angle becomes imaginary when the sum resonance dominates ($|w_+| > |w_-|$) in agreement with Y.Luo's results [6].

APPENDIX B. TUNE EVALUATION FROM TBT DATA

Let us first introduce continuous Fourier transform (CFT) and its inverse:

$$\begin{aligned} &X(\nu) = \frac{1}{N}\sum_{n=1}^{N} e^{-2\pi i\nu(n-1)} x_n, \\ &x_n = N\int_0^1 e^{2\pi i\nu(n-1)} X(\nu) d\nu. \end{aligned} \tag{B.1}$$

For harmonic oscillations, $x_{n+1} = a\cos(2\pi\nu_0 n + \psi)$, the transform is

$$X(\nu) = \frac{a}{2}[e^{-\pi i(\nu-\nu_0)(N-1)+i\psi} F(\nu-\nu_0) + e^{-\pi i(\nu+\nu_0)(N-1)-i\psi} F(\nu+\nu_0)], \tag{B.2}$$

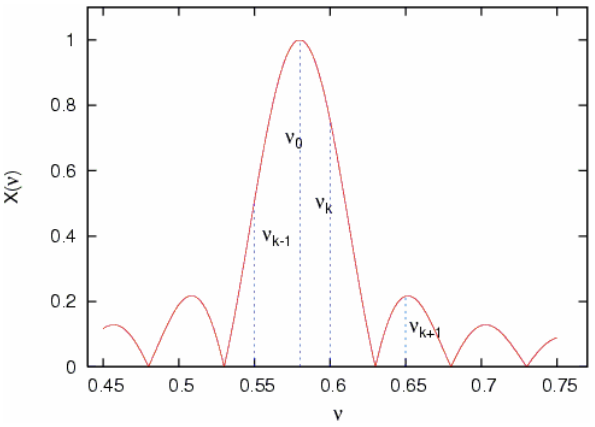

FIG. 7. Schematic of TBT spectrum and sampling points for discrete Fourier transform.

where

$$F(\nu) = \frac{\sin \pi\nu N}{N \sin \pi\nu}. \tag{B.3}$$

Discrete Fourier transform picks up $X(\nu)$ values at $\nu = \nu_k \equiv (k-1)/N$ (see Fig.7). The simplest estimate of the tune (1-point formula) is $\nu_0 = \nu_k$ with k corresponding to the maximum value of $X_k = |X(\nu_k)|$. The error of such estimate is ~$1/N$.

One may try to fit the TBT spectrum using model spectral function

$$S(\nu_k) = \frac{a}{2} | F(\nu_k - \nu_0) | \tag{B.4}$$

Since the model contains just two parameters, a and ν_0, just two Fourier components X_k are necessary. Choosing the largest two and assuming $\nu_{k-1} < \nu_0 \le \nu_k$ we obtain the 2-point formula first derived by E.Asseo (see Ref.[15]):

$$\nu_0 = \nu_k - \frac{1}{\pi} \arctan \frac{X_{k-1} \sin(\pi/N)}{X_k + X_{k-1} \cos(\pi/N)}. \tag{B.5}$$

Even in the case of harmonic oscillations this formula is not exact since model (B.4) does not include the contribution from the mirror-symmetric peak, the error being ~$1/N^2$. The accuracy may become significantly worse in the presence of alien spectral lines (e.g. synchrotron sidebands) and random noise. For instance, if their contribution is large enough to make X_{k+1} higher than X_{k-1} in the situation depicted in Fig.7 then the calculated tune will lie on the wrong side of ν_k resulting in an error ~$1/N$.

To reduce sensitivity of the method (called interpolated FFT) to the noise one may try to use more points, e.g. three with the highest peak in the middle. Since only two points are really necessary there is no unique expression; we offer the following formula

$$\nu_0 = \nu_k + \frac{\mathrm{sign}(X_{k+1} - X_{k-1})}{\pi} \arctan \frac{2X_{k-1}X_{k+1} \sin(\pi/N)}{X_k (X_{k+1} + X_{k-1})}. \tag{B.6}$$

Let us compare its precision with the 2-point formula in the case of signal contamination with an alien mode assuming for simplicity $\nu_0 = \nu_k \equiv (k-1)/N$:

$$x_{n+1} = \cos(2\pi\nu_k n) + \varepsilon \cos(2\pi\nu_a n). \tag{B.7}$$

Retaining only the first order correction in ε we get for the tune error $\delta\nu_0$ from eq. (B.5)

$$|\tan \pi\delta\nu_0| = \frac{\varepsilon}{N} \frac{|\sin N\pi\Delta| \sin(\pi/N)}{\sin[\pi(|\Delta| - 1/N)]} \approx \frac{\pi\varepsilon}{N^2} \frac{2}{\pi^2|\Delta|}, \tag{B.8}$$

where $\Delta = \nu_a - \nu_0$, while from the 3-point formula (B.6) we obtain

$$\left|\tan \pi\delta\nu_0\right| = \frac{\varepsilon}{N}\tan\frac{\pi}{N} \approx \frac{\pi\varepsilon}{N^2} \tag{B.9}$$

independently of Δ. With typical distance to the alien lines $\Delta=10^{-3}\div10^{-2}$ the error of the 2-point formula can be by one-two orders of magnitude larger than that of the 3-point formula.

Unfortunately, the 3-point algorithm fails as well when the sign of $X_{k+1} - X_{k-1}$ is reversed by noise. So the most reliable method of tune evaluation is finding the maximum of CFT.

APPENDIX C. ERRORS DUE TO RANDOM NOISE

Let us consider the effect of random uncorrelated errors (e.g. LSB)

$$x_{n+1} = a\cos(2\pi\nu_0 n + \psi) + \xi_{n+1}, \quad \langle \xi_n \xi_m \rangle = \sigma^2 \delta_{mn}, \tag{C.1}$$

on the precision of determination of tune, amplitude and phase by continuous Fourier transform. For tunes sufficiently far from half-integer values the second term in eq.(B.2) can be dropped and we have at small tune deviations $\Delta=\nu - \nu_0$

$$X(\nu) = \frac{a}{2}e^{i\psi}[1-\pi i(N-1)\Delta - \frac{\pi^2(2N^2-3N+1)}{3}\Delta^2] + \frac{1}{N}\sum_{n=1}^{N} e^{-2\pi i(n-1)\nu_0}[1-2\pi i(n-1)\Delta]\xi_n\,. \tag{C.2}$$

Maximum of $|X(\nu)|$ is reached at

$$\Delta = \frac{6}{\pi N(N^2-1)a^2}\sum_{n=1}^{N}(N+1-2n)\sin[2\pi\nu_0(n-1)+\psi]\xi_n\,, \tag{C.3}$$

so the r.m.s. tune error is

$$\sigma_\nu = \sqrt{<\Delta^2>} \approx \frac{\sqrt{6}\sigma}{\pi N^{3/2} a} \tag{C.4}$$

R.m.s. errors in amplitude and phase of $X(\nu_0)$ are

$$\begin{aligned} \sigma_a &= \sqrt{<[2\left|X(\nu_0)\right| - a]^2>} \approx \frac{\sqrt{2}\sigma}{N^{1/2}}, \\ \sigma_\psi &= \sqrt{<\arg^2 X(\nu_0)>} \approx \frac{\sqrt{2}\sigma}{N^{1/2}a}. \end{aligned} \tag{C.5}$$

Errors due to random noise decrease with the number of turns N much slower than errors due to alien modes, Hanning windowing does not reduce them.

APPENDIX D. TUNES OF COUPLED OSCILLATIONS

In the case when functions $C_\pm(\theta)$ defined in eq.(A.27) contain only one harmonic each:

$$C_\pm(\theta) = c_\pm e^{-in_\pm\theta}, \tag{D.1}$$

it is possible to find the coupled tunes exactly.

Introducing new variables

$$b_x = a_x \exp(-i\frac{n_+ + n_-}{2}\theta), \quad b_y = a_y \exp(-i\frac{n_+ - n_-}{2}\theta), \tag{D.2}$$

we get from eqs.(2.21), (2.24) and (A.26) equations of motion with constant coefficients

$$\begin{aligned} \dot{b}_x &= iq_x b_x + \frac{i}{2}c_+^* b_y^* + \frac{i}{2}c_-^* b_y, \\ \dot{b}_y &= iq_y b_y + \frac{i}{2}c_+^* b_x^* + \frac{i}{2}c_- b_x, \end{aligned} \tag{D.3}$$

where $q_{x,y} = Q_{x,y0} - (n_+ \pm n_-)/2$.

Eqs.(D.3) and their complex conjugates present a system of four equations for the components of vector $\underline{b} = (b_x, b_x^*, b_y, b_y^*)$. Finding the particular solutions we may ignore the requirement of b_n, b_n^* being complex conjugates but satisfy it later in the global solution.

Looking for $\underline{b} \sim \exp(iq\theta)$ we find four eigenvalues

$$\begin{aligned} q_{1,2}^2 &= \frac{1}{2}(q_x^2 + q_y^2) - \frac{1}{4}\left|c_+^2\right| + \frac{1}{4}\left|c_-^2\right| \pm \frac{1}{2}\sqrt{(q_x^2 - q_y^2)^2 - (q_x - q_y)^2\left|c_+^2\right| + (q_x + q_y)^2\left|c_-^2\right|}, \\ q_{3,4} &= -q_{1,2}. \end{aligned} \tag{D.4}$$

When either $c_+ = 0$ or $c_- = 0$ we obtain well known results

$$\begin{aligned} q_{1,2}^2 &= \frac{1}{4}[q_x + q_y \pm \sqrt{(q_x - q_y)^2 + \left|c_-^2\right|}]^2, \quad c_+ = 0, \\ q_{1,2}^2 &= \frac{1}{4}[q_x - q_y \pm \sqrt{(q_x + q_y)^2 - \left|c_+^2\right|}]^2, \quad c_- = 0. \end{aligned} \tag{D.5}$$

The effect of c_+ on the tune difference (as well as that of c_- on the tune sum) is small,

$$q_1 - q_2 = \sqrt{(q_x - q_y)^2 + \left|c_-^2\right|} \times \left\{1 + \frac{\left|c_+^2 c_-^2\right|}{2(4q_x q_y - \left|c_-^2\right|)[(q_x - q_y)^2 + \left|c_-^2\right|]} + \ldots\right\}, \tag{D.6}$$

and can be ignored in practical calculations as has been done in eq.(4.15)

References

1. V.Lebedev, V.Sajaev, in *Proceedings of the PAC 2005, Knoxville, TN* (to be published).
2. R.Tomas, Phys. Rev. ST Accel. Beams **5**, 054001 (2002).
3. X.Huang, S.Y.Lee, E.Prebys and R.Tomlin, in *Proceedings of the PAC 2005, Knoxville, TN* (to be published).
4. D.Sagan, D.Rubin, Phys. Rev. ST Accel. Beams **2**, 074001 (1999).
5. W.Fischer, Phys. Rev. ST Accel. Beams **6**, 062801 (2003).
6. Y.Luo, BNL C-AD/AP Note 187, 2005 (unpublished).
7. D.Edwards, L.Teng, IEEE Trans. NS **20**, N 3, pp.885-889 (1973).
8. H.Mais, G.Ripken, DESY M-82-05, 1982 (unpublished).

9. F.Willeke, G.Ripken, *Methods of Beam Optics*, in AIP Conf. Proc. **184**, 758 (1989).

10. G.Guignard, J.Hagel, *Hamiltonian Treatment of Betatron Coupling*, in CERN 92-01, 62 (1992).

11. L.Michelotti, *Intermediate Classical Dynamics with Applications to Beam Physics*, (John Wiley & Sons, Inc., New York, 1995).

12. V.Lebedev, S.Bogacz, *Betatron motion with coupling of horizontal and vertical degrees of freedom*, http://www-bdnew.fnal.gov/pbar/organizationalchart/lebedev/Articles/index.htm

13. P. Castro-Garcia, Ph.D. Thesis, CERN-SL-96-70-BI (1996).

14. J.R.Cary, *Lie Transform Perturbation Theory for Hamiltonian Systems, Physics Reports*, **79**, No.2 (1981).

15. R.Bartolini, A.Bazzani, M.Giovannozzi, W.Scandale and E.Todesco, Particle Accelerators, **56**, 167-199 (1996)